

Seismic Response of Geosynthetic Reinforced Earth Embankment by Centrifuge Shaking Table Tests

W.Y. Hung¹, J.H. Hwang², C.J. Lee³

¹Assistant Professor, Dept. of Civil Engineering, National Central University, Taiwan

²Professor, Dept. of Civil Engineering, National Central University, Taiwan

³Professor, Dept. of Civil Engineering, National Central University, Taiwan

¹E-mail: wyhung@ncu.edu.tw

²E-mail: hwangjin@cc.ncu.edu.tw

³E-mail: cjleeciv@ncu.edu.tw

ABSTRACT: The advantages of reinforced earth structures are their flexibility and capability to absorb deformations due to poor foundation and seismic loadings. In this study, 7 centrifuge shaking table tests were performed to investigate the effect of reinforcement arrangement on seismic response of geosynthetic reinforced earth embankment. The test results show that the natural frequency of an 8 m-high GRE embankment is about 5.7Hz. The arrangement of reinforcement and the inclination of slope facing do not affect the natural frequency significantly. The amplification of acceleration increases with the increasing elevation and the increasing frequency of input motion. If the embankment has enough reinforcement strength, the reinforcement spacing and the inclination of slope facing would not affect the settlement significantly. Insufficient reinforcement strength would lead to internal instability failure and a large settlement. The external instability would occur for the embankment using too short reinforcement length.

KEYWORDS: Centrifuge shaking table test, geosynthetic reinforced earth embankment, natural frequency

1. GENERAL INSTRUCTIONS

Taiwan is an island with limited area but dense population. It is a key issue to improve the transportation system with minimal impact on the local ecosystems. Engineers integrate eco-technology into road construction projects for finding solutions to promote a safe and ecological transportation infrastructure while conserving biodiversity and sustainable development. Therefore, geosynthetic reinforced earth (GRE) structures were introduced into Taiwan and usually used for retaining soils as they are aesthetically attractive and more ecologically sound to the local environment.

Reinforced earth consists of soil backfill and man-made materials, called reinforcements, such as metal strips, geosynthetic sheets or grids. The reinforcements sustain the forces resulting from the structure deformation and the external loadings. The most advantages of GRE structures, as compared with the reinforced concrete structures, are their flexibility and capability to absorb deformation due to poor foundation and seismic loadings. Several centrifuge modeling tests were performed by Viswanadham and Kong (2009) to investigate the effect of differential settlement of foundation on the reinforced earth slope with flexible facing. The test results indicated that even after inducing a differential settlement equivalent to 1.0 m in prototype dimensions, the reinforced soil structure was not found to experience a collapse failure.

In addition, the observations made after Chi-Chi earthquake of Taiwan (Ling et al., 2001) or Hanshin-Awaji earthquake of Japan (Lee, 1997) showed that most of the reinforced soil structures survived without serious damages, demonstrating their capability to resist the earthquakes. The seismic behaviour of reinforced earth wall and slope were studied by Nova-Roessig and Sitar (2006) using centrifuge shaking table. The models were subjected to maximum input accelerations of up to 1.08g. The experimental results show that reinforced slope moves under small input motions, and significant lateral and vertical deformations occur under strong shaking. But the distinct internal failure surface was not observed. The magnitude of deformations is related to the backfill density, reinforcement properties, arrangement of reinforcement and geometry of reinforced earth structure.

From the other past studies (Hu et al., 2010; Chen et al., 2007), it was also found that the properties and arrangement of reinforcement including length, spacing, and strength affects the deformation of

GRE structures significantly. Therefore, 7 centrifuge shaking table tests were performed to investigate the effect of reinforcement spacing and inclination of slope facing on the seismic response of geosynthetic reinforced earth (GRE) embankment, including the natural frequency, the amplification of acceleration and the settlement on the top. A very weak reinforcement material with different length was used for three models to find the effect on the deformation of structure after a series shaking events.

2. EQUIPMENT AND TEST PREPERATION

2.1 Geotechnical centrifuge and materials

This experimental work was undertaken in the centrifuge modelling laboratory at the National Central University (NCU). The NCU centrifuge has a nominal radius of 3 m and a 1-D servo-hydraulically controlled shaker is equipped into a swing basket. The NCU centrifuge, the shaking table and the rigid model container are shown in Figure 1. The shaker has maximum nominal shaking force of 53.4 kN with maximum table displacement of ± 6.4 mm at 80 g centrifugal acceleration. The nominal operating frequency ranges from 0 Hz to 250 Hz. A rigid model container with inside dimensions of 767 mm x 355 mm x 400 mm (L x W x H) is used for dry or saturated soil models.

A fine clean uniform quartz sand was adopted to prepare sandy models by dry pluviation method. The quartz sand was pluviated into the rigid model container with a regular path, a constant flow rate and fixed drop height. The fundamental properties of quartz sand are summarized in Table 1. The mean particle size is 0.19 mm which is finer than the usual sand soil to avoid the particle effects in centrifuge modelling test.

On the other hand, it is very important to determine the scaling factor of reinforcement strength in performing the centrifuge modeling test for GRE structure. Law et al. (1992) used eight centrifuge experiments with 1/5-scale models to predict the response of full scale geosynthetic reinforced retaining walls. Wall movement was monitored continuously by the linear variation deferential transformers (LVDTs) during the test in which a surcharge pressure was applied incrementally under 5 g acceleration. It was found that the model with reinforcement strength not scaled gave results close to the observed deformation of prototype before failure.



(a)



(b)

Figure 1 (a) NCU geotechnical centrifuge; (b) The shaking table and rigid container

Table 1 The fundamental properties of quartz sand

Properties	Quartz sand
Mean size, D_{50} (mm)	0.19
Effective size, D_{10} (mm)	0.15
Maximum dry unit weight, $\gamma_{d,max}$ (kN/m ³)	16.3
Minimum dry unit weight, $\gamma_{d,min}$ (kN/m ³)	14.1
Specific gravity, G_s	2.65
Friction angle, ψ (Dr=40%) (degree)	35
Unified soil classification system	SP

Lord Jr. (1987) analyzed a geosynthetic reinforced slope by limit equilibrium analysis, and the dimensional analysis was applied to the resulting equations. It gave the scaling factor of reinforcement strength/unit length as $1/N^2$, where N is the artificial acceleration by centrifuge. The scaling laws governing the behaviour of cohesionless reinforced soil slopes at failure were also derived by Zornberg et al. (1997, 1998) based on the requirement that both the prototype and scaled model have the same factor of safety which was calculated as the ratio of moments resisting slope failure to that driving slope failure. Assumed a circular failure surface, the scaling factor of reinforcement strength was equal to $1/N$. It should be noted that the difference between Zornberg's and Lord's results lies in whether the width dimension of the GRE structure was taken into consideration or not.

Zhang et al. (2000) used the relations $E_m(N^2 A_m) = E_p A_p$ and $N T_m = T_p$, to scale the stiffness and the strength of reinforcement, where E is the elastic modulus of reinforcement, A is the cross sectional area of reinforcement, T is the unit tensile strength of reinforcement, and the subscripts m and p indicate the model and the prototype, respectively. However, Leshchinsky and Han (2004) used the numerical analysis program, FLAC, to show that the reinforcement stiffness does not play an important role if the reinforcement strength was adequate and the global stability of wall was concerned. It should be noted that the limit equilibrium analysis can't consider the influences of reinforcement stiffness but the continuum mechanics-based analysis program used in the study. The use of limit equilibrium analysis yields nearly the same factors of safety against collapse as the continuum mechanics-based analysis. The result thus implies that for evaluating the global stability a wall system reinforced with different reinforcement

stiffness, such as metal or geosynthetic, can be analyzed by the use of limit equilibrium analysis.

Amid these conflicting results for the scaling factor of reinforcement strength, the concept of modeling of models was adopted by Hung (2008) to clarify how the reinforcement strength should be scaled in the centrifuge modeling tests. It was found that the reinforcement strength needs to be scaled indeed for simulating a corresponding prototype, and the scaling factor of reinforcement strength at internal instability failure is $1/N$. Therefore, two very weak geosynthetic material with tensile strengths of 2.24 kN/m and 0.05 kN/m were selected to simulate the prototype reinforcement material with strength of 112.0 kN/m and 2.5 kN/m, respectively, in 50 g acceleration field.

2.2 Model setup

All the models in this study were wrapped-face, sandy backfill and using the 100% coverage rate of reinforcement material and tested in 50 g acceleration field. The purpose of this study was to investigate the effect of reinforcement spacing and face inclination on the seismic response of GRE embankment and the internal failure surface induced by different input motions. In the design of GRE embankment models, it must be ensured that (1) the external instabilities including sliding, overturning and bearing capacity failure do not occur (2) the internal instability of pull-out failure does not occur. Consequently, a teeth-shape aluminium alloy plate was installed at the bottom of rigid model container to avoid sliding of the model during shaking. Above the teeth-shape plate, the sandy foundation is firm and only 10 mm thick.

The foundational properties of GRE embankment models are shown in Table 2 in prototype scale. The tested modes were labelled according to the face inclination, number of reinforcement layers, reinforcement strength and reinforcement length and separated by hyphens. The height and the width at the top of GRE embankment models are 160 mm and a 367 mm, respectively, to simulate the prototype embankments with 8 m-high and 18.35 m-wide in 50 g. The reinforcement length is 0.71 times of height and the overlap length is 0.4 times of reinforcement length as shown in Two face inclinations were chosen with slope of 1.0:1.0 (Figure 2 vertical: horizontal) and 1.0:0.5 (vertical: horizontal). Based to the design guidelines, the reinforcement spacing was not allowed to be larger than 0.8 m and a spacing of 0.5 m was usually used in practice. Hung (2008) suggested that the ratio of reinforcement spacing to sand mean particle size (s_{vm}/d_{50}) should be larger than 43 to avoid the local failure of GRE wall resulting from the particle effect. Therefore, two reinforcement spacings of 16 mm and 10 mm were adopted with corresponding to the s_{vm}/d_{50} values of 84.2 and 52.6, respectively.

Table 2 The fundamental properties of tested models

Test No.	W* (m)	H** (m)	Inclination	s_v *** (m)	T_u **** (kN/m)
1:1-N10-T112-L70	18.35	8.0	1:1.0	0.8	112.0
1:0.5-N10- T112-L70	18.35	8.0	1:0.5	0.8	112.0
1:1-N16- T112-L70	18.35	8.0	1:1.0	0.5	112.0
1:0.5-N16- T112-L70	18.35	8.0	1:0.5	0.5	112.0
1:0.5-N10-T2.5-L30	18.35	8.0	1:0.5	0.8	2.5
1:0.5-N10- T2.5-L50	18.35	8.0	1:0.5	0.8	2.5
1:0.5-N10- T2.5-L70	18.35	8.0	1:0.5	0.8	2.5

* W is the width at the top GRE embankment

** H is the height of GRE embankment

*** s_v is the reinforcement spacing

**** T_u is the reinforcement strength

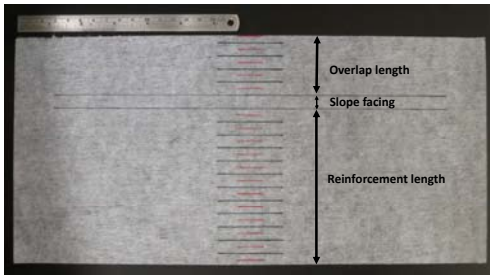
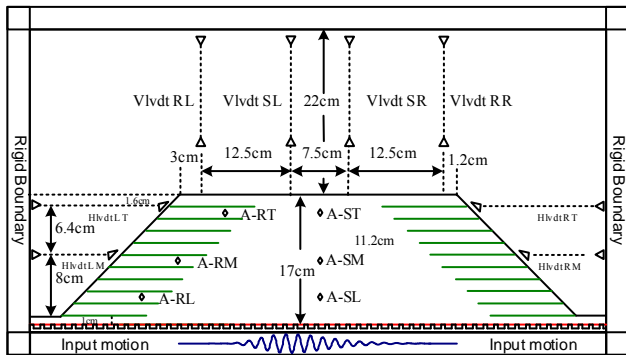
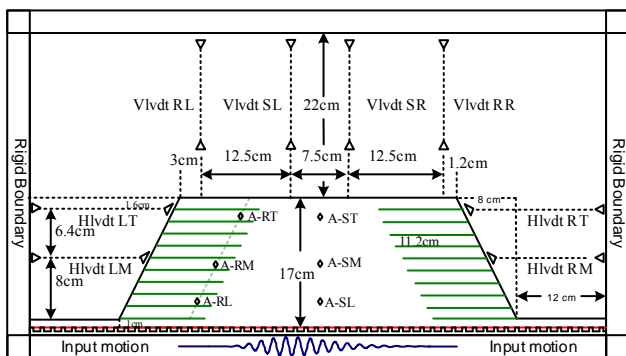


Figure 2 The top view of reinforcement material

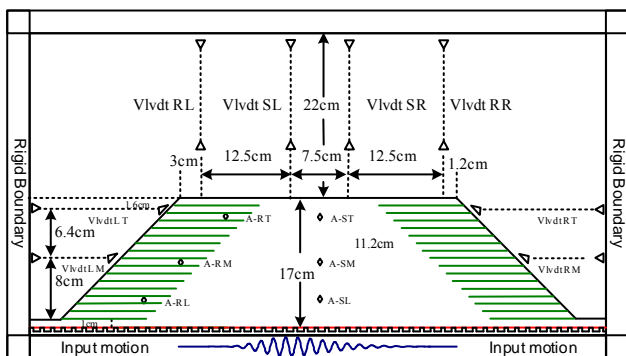
Figures 3(a) to 3(g) show the profile and the arrangement of sensors for seven models. For each model, seven accelerometers were installed including one fixed on the shaking table to monitor the input motion.



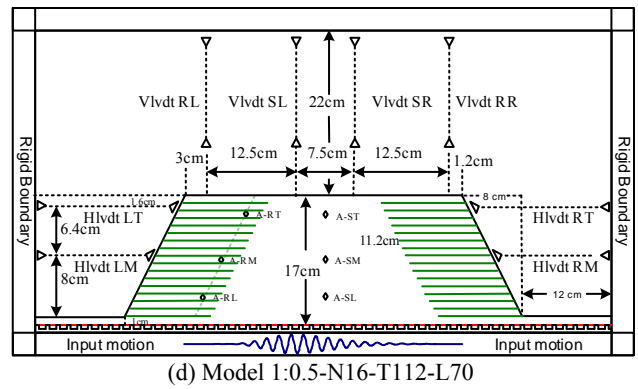
(a) Model 1:1-N10-T112-L70



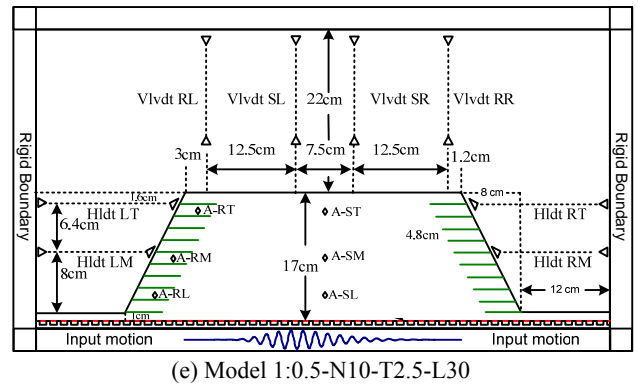
(b) Model 1:0.5-N10-T112-L70



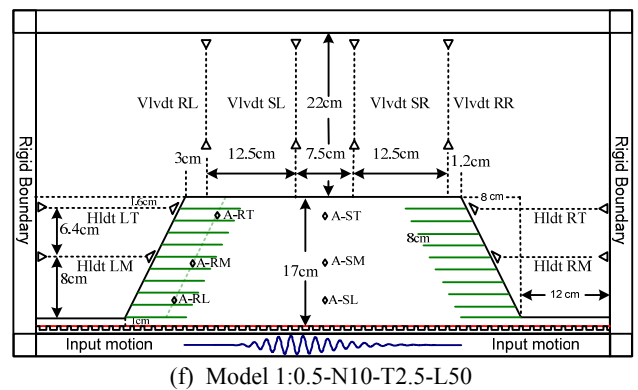
(c) Model 1:1-N16-T112-L70



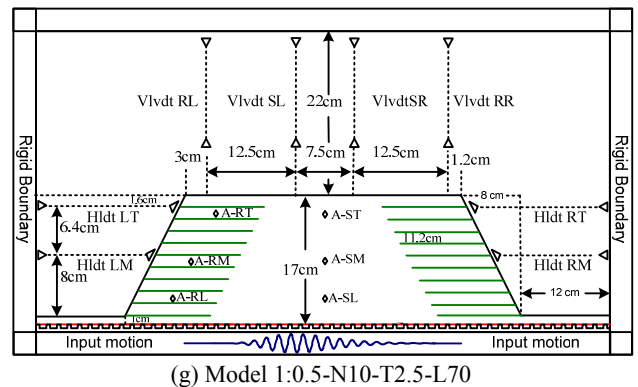
(d) Model 1:0.5-N16-T112-L70



(e) Model 1:0.5-N10-T2.5-L30



(f) Model 1:0.5-N10-T2.5-L50



(g) Model 1:0.5-N10-T2.5-L70

Figure 3 The profile and sensors arrangement for tested models

Two accelerometer arrays were inside the retained soil zone (A-ST, A-SM, A-SL) and the reinforced earth zone (A-RT, A-RM, A-RL), respectively. 4 LVDTs were placed on the top of embankment to measure the vertical settlement labelled as Vlvdt RL, Vlvdt SL, Vlvdt SR and Vlvdt RR. The other 4 LVDTs were fixed at the elevation of 8 cm and 14.4 cm above the ground surface to measure the horizontal displacement of slope facing, labelled as Hlvdt LT, Hlvdt LM, Hlvdt RT and Hlvdt RM. In the following figures in this paper, the notations of SZ, RZ and Base represent the retained soil zone, reinforced earth zone and input motion, respectively.

Before constructing the model, the rigid model container was put on a trolley, set on the base of the traveling pluviation apparatus and raised to the appropriate height by hydraulic jack. The sand was pluviated into the container with a constant drop height. During the construction of GRE embankment model, several pieces of hard styrofoam boards were piled up in front of the model to provide lateral supports during construction. For each reinforcement layer, the reinforcement material was placed firstly and the sand was then pluviated until the desired reinforcement spacing was reached. The accelerometers were placed at the proper position inside the model simultaneously. Then, the reinforcement was wrapped to produce slope facing and embedded into the backfill. This process was repeated until it reached the designed height. Figure 4(a) shows the completed GRE embankment model with lateral supports. After removing away the hard styrofoam boards, the inclined facing was done as indicated in Figure 4(b).

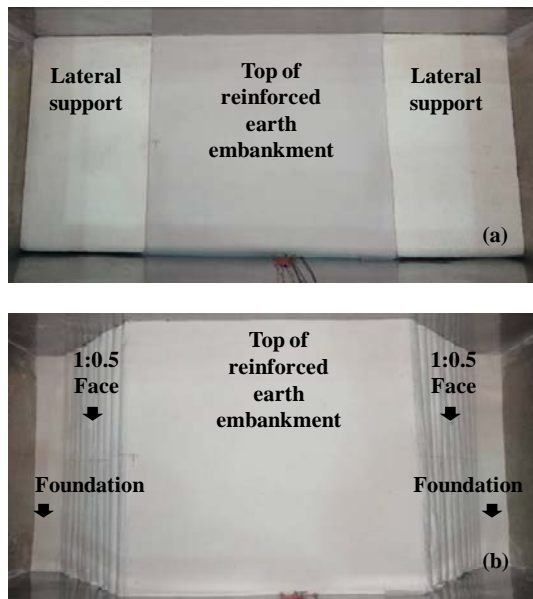


Figure 4 The completed GRE embankment model: (a) with lateral supports; (b) removing away the lateral supports

Finally, the weight of model was measured to check the relative density. Four LVDTs were instrumented on the top of embankment to measure the vertical settlement as indicated in Figure 5(a).

Four LVDTs were setup in front of the each side to monitor the horizontal displacements at the crest and the middle of slope facing as shown in Figure 5(b). The completed model was then put on the centrifuge platform and fixed on the shaking table to start the centrifuge modeling processes.

2.3 Testing Procedures

The completed model was accelerated step by step to 50 g, where the increment of acceleration in each step is 10g. The model was maintained and lasted for 3 minutes at each step to ensure the consolidation of sand model. At 50 g, the model was then excited with a series of one-dimensional seismic events. Firstly, white noise input motion was applied to detect the natural frequency of the GRE embankment system. Then, two series of seismic events were applied to the models with sinusoid base input motion consisting of 15 cycles. In the first series, the frequency of input motions was 1 Hz (in prototype) and the average base input acceleration were about 0.08 g, 0.12 g and 0.23 g (in prototype), respectively. For instance, the right figures in Figures 6(a), 6(b) and 6(c) are acceleration time histories of base input motions, and the left figures are the responses of acceleration at the top of reinforced earth zone.

In the second series of test, the higher frequency of base input motion was selected. Based on the nominal operating frequency range of NCU shaking table, the frequency of 240 Hz was adopted which was 4.8 Hz in prototype. The average base input acceleration were about 0.03 g, 0.06 g and 0.11 g (in prototype), respectively. The right figures in Figures 7(a), 7(b) and 7(c) are the acceleration time histories of base input motions, and the left figures are the responses of acceleration at the top of reinforced earth zone.

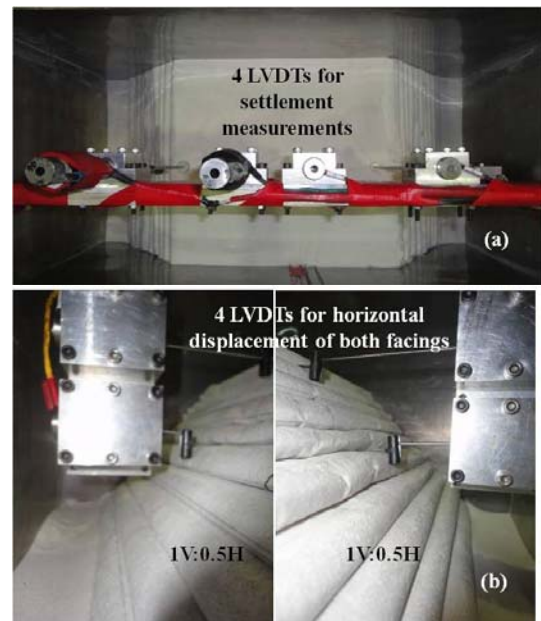


Figure 5 The installation of LVDTs: (a) for settlements; (b) for horizontal displacements of both facings.

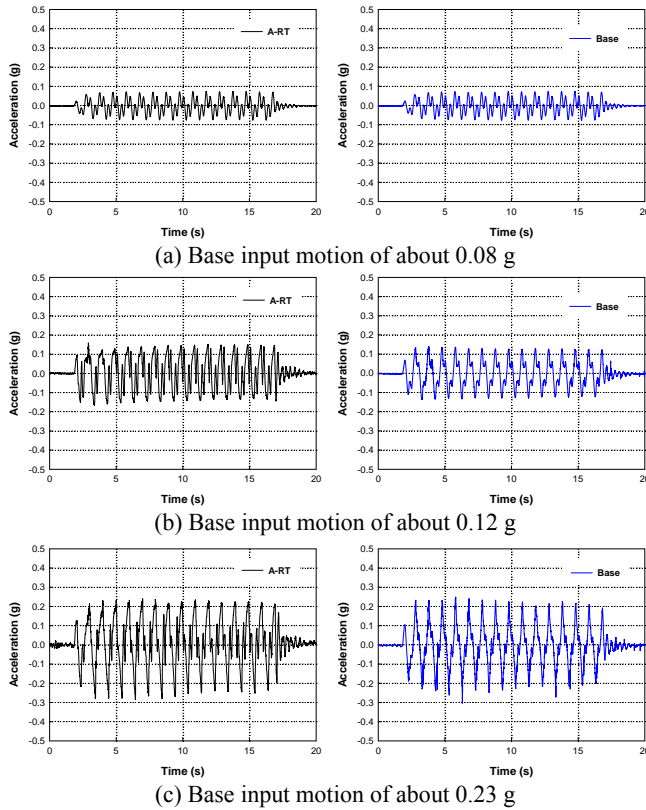


Figure 6 Acceleration time histories of different amplitude input motions with frequency of 1 Hz

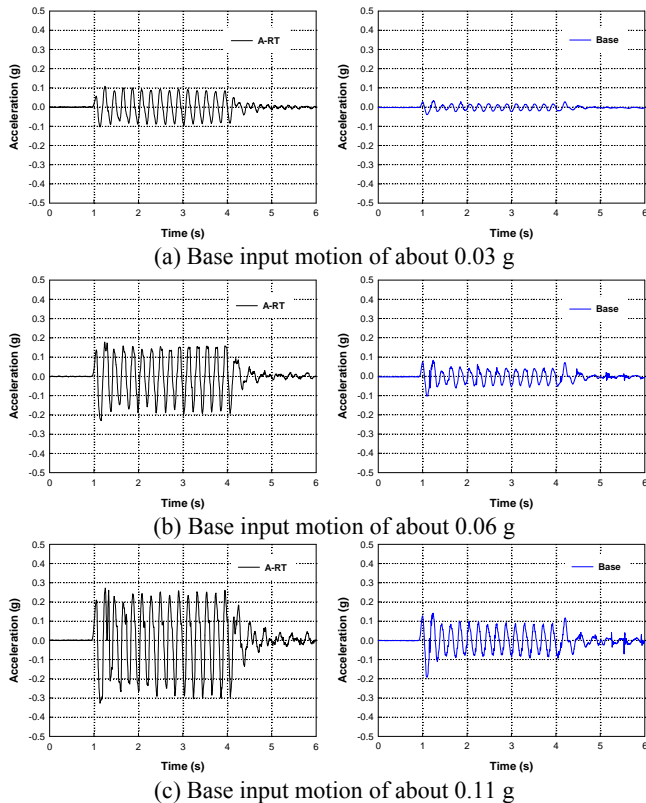


Figure 7 Acceleration time histories of different amplitude input motions with frequency of 4.8 Hz

3. TEST RESULT AND ANALYSIS

3.1 Natural Frequency of GRE Embankment

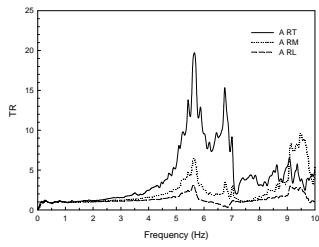
From the past studies, it was concluded that the arrangement of reinforcement affects the stability of GRE structures. Thus, seven GRE embankment models were conducted to understand the effect of reinforcement spacing, inclination of slope facing, reinforcement strength and reinforcement length on the natural frequency of system. The acceleration histories obtained from the white noise input motion were adopted and transformed to frequency domain by Fast Fourier Transform (FFT). Then, the Fourier spectrum of each accelerometer divided by that of input motion was transfer function (TR) which was the amplification of acceleration at different frequency. The frequency at the first peak of transfer function is the natural frequency of system. Figures 8(a) to 8(g) are the transfer functions got from the retained soil zone. They indicate that the first and the second peaks are about 5.7 Hz and 6.8 Hz, which may be resulting from the interaction of retained soil zone and reinforced earth zone and need more investigations to clarify. Table 3 summarizes the results including the natural frequencies of reinforced earth zone and retained soil zone and the relative density of GRE embankment. From the tests, the relative density, reinforcement strength, reinforcement length, inclination of slope facing and reinforcement spacing were altered, the natural frequencies of GRE embankments changed slightly from 5.2 to 5.7. It means that these parameters do not affect the natural frequency of GRE embankment significantly. The natural frequency for a GRE embankment with height of 8 m and top width of 18.35 m is about 5.7 Hz. The effects of top width and height on the seismic response of GRE embankment would need advanced studies.

On the other hand, it can be seen that the values of transfer function at 1 Hz for different positions inside the GRE embankment are close to 1, illustrating that the acceleration is not amplified at the input motion of 1 Hz. At frequency of 4.8 Hz, the transfer function changes significantly at different elevations leading to different amplification of acceleration response. But the relationships between the amplification and the elevation inside the GRE embankment are not regular and clear from this figure. In the following section, the amplifications of acceleration are calculated directly from the peaks of acceleration histories at different seismic events.

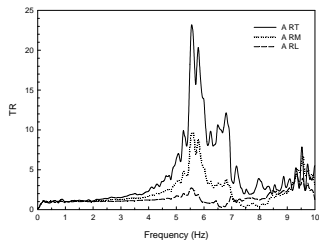
3.2 Amplification of Acceleration of GRE Embankment

As shown in Figures 6 and 7, though the amplitudes of 1 Hz and 4.8 Hz base input motions are significantly different, the peak accelerations measured at the same elevation are almost the same. The base input motions of 1 Hz frequency are about 0.08 g, 0.12 g and 0.23 g, and those of 4.8 Hz are about 0.03 g, 0.06 g and 0.11 g. The peak accelerations are 0.09 g, 0.13 g and 0.25 g, respectively, measured at the bottom, medium and top of GRE embankment. Therefore, the amplifications were calculated from the peaks of acceleration histories. The main shaking events were sinusoidal waves with 15 cycles and there are 30 peak values for each accelerometer in a seismic event including the positive and negative data. The absolute peak values of acceleration histories measured from the retained soil zone and the reinforced earth zone are calculated and plotted. Figures 9 and 10 are the results of retained soil zone and reinforced earth zone. These figures show the relationships between input base accelerations (x axis) and response accelerations (y axis) at the top, medium and bottom of GRE embankment, respectively. In these figures, black and grey squares are the peaks of accelerations for 1 Hz and 4.8 Hz input motions, respectively. The black line indicates that the peak of input motion is equal to the measured acceleration. If the symbols locate at the left side of black line, meaning that the acceleration is amplified. However, the black squares in each figure locate on a trend which is closer to the black line than that of grey squares. It seems that the arrangement of reinforcement material and the designed inclination

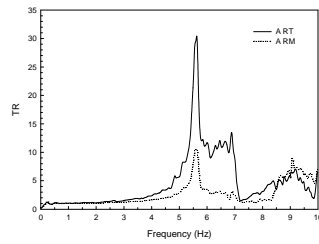
of slope facing in this study do not affect the amplification of acceleration significantly while the GRE embankment subjected to 1 Hz seismic loadings.



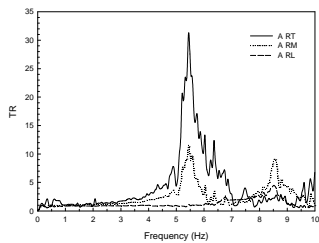
(a) 1:1-N10-T112-L70



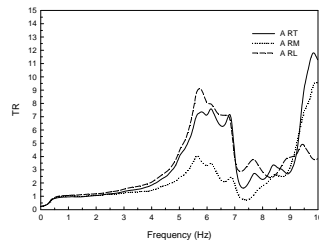
(b) 1:0.5-N10-T112-L70



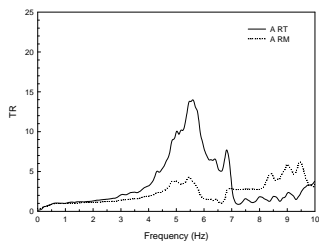
(c) 1:1-N16-T112-L70



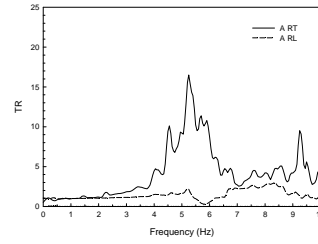
(d) 1:0.5-N16-T112-L70



(e) 1:0.5-N10-T2.5-L30



(f) 1:0.5-N10-T2.5-L50

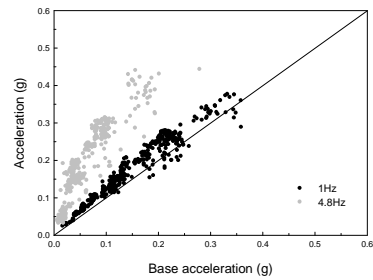


(g) 1:0.5-N10-T2.5-L70

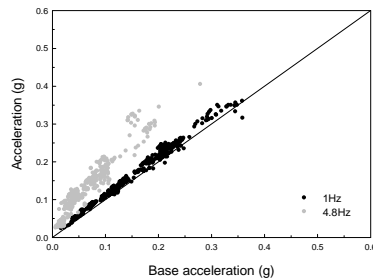
Figure 8 Transfer functions of retained soil zone at different elevation for seven models

Table 3 The natural frequency of seven models

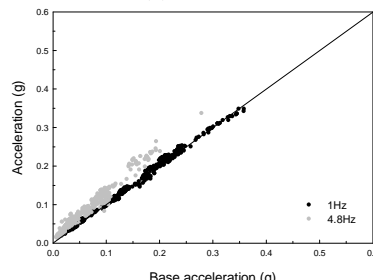
Test No.	D_r (%)	Natural frequency (Hz)	
		Reinforced earth zone	Retained soil zone
1:1-N10-T112-L70	77.3	5.7	5.6
1:0.5-N10-T112-L70	67.0	5.6	5.6
1:1-N16-T112-L70	66.2	5.6	5.6
1:0.5-N16-T112-L70	53.3	5.5	5.4
1:0.5-N10-T2.5-L30	53.3	5.6	5.7
1:0.5-N10-T2.5-L50	53.3	5.6	5.4
1:0.5-N10-T2.5-L70	53.3	5.2	5.2



(a) Top



(b) Medium



(c) Bottom

Figure 9 Relationships of input base accelerations and response accelerations of retained soil zone at the different elevation

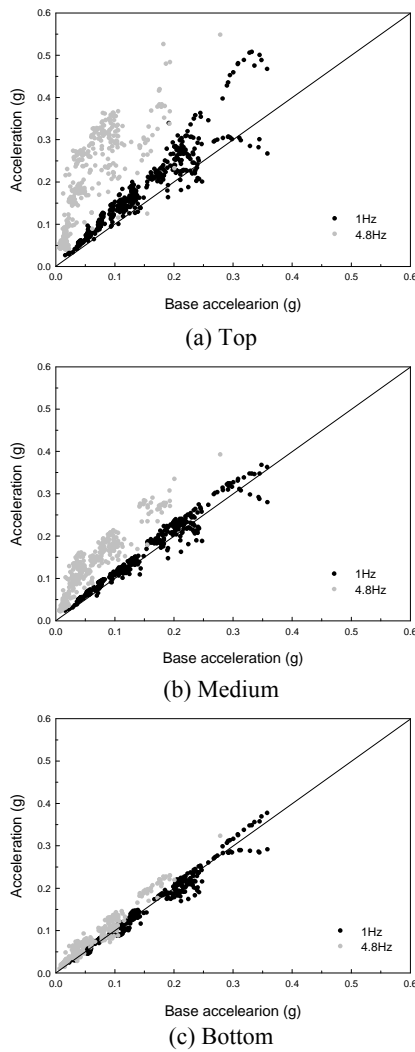


Figure 10 Relationships of input base accelerations and response accelerations of reinforced earth zone at the different elevation

For GRE embankment subjected to 4.8 Hz seismic loadings, the amplifications inside the reinforced earth zone are slightly larger than those inside the retained earth zone. Accelerations are amplified significantly with increasing elevation inside either the retained soil zone or the reinforced earth zone. The grey squares almost locates on a steeper for GRE embankment is not highly related to the arrangement trend and this linear relationships show that the response of acceleration of reinforcement material and the designed inclination of slope facing in this study. According to Figures 9 and 10, the relationships of normalized elevation by height and mean values of amplification w drew in Figures 11(a) and 11(b). The hollow symbols are graded to three input motions with frequency of 1 Hz. They are relatively small, middle and large accelerations with corresponding to the mean base input accelerations of 0.056 g, 0.111 g and 0.199 g, which are labelled as hollow circular, square and triangle, respectively. It can be seen that the mean amplifications increase slightly with increasing elevation inside either the retained soil zone or the reinforced earth zone. The maximum amplification of acceleration is about 1.3 at the top of retained soil zone for an 8 m-high GRE embankment subjected to 1 Hz and about 0.056 g seismic loadings. The solid symbols are also graded to three input motions with frequency of 4.8 Hz. The mean input accelerations are 0.015 g, 0.037 g and 0.086 g and labelled as solid circular, square and triangle, respectively. It can be observed that the mean amplification increases dramatically with increasing elevation for input motion with frequency of 4.8 Hz. The maximum

amplification of acceleration at the top is about 5.7 for input motion of 0.037 g. Current GRS structure design guidelines (i.e., Elias et al. 2001; NCMA 2010) conventionally assume the response acceleration is uniformly distributed with height. The influences of elevation of embankment and frequency of input motion on amplification are not considered in the current design guidelines. Consequently, if a constant acceleration is used to design a GRE embankment, the design results would underestimate the seismic response at the top portion of the GRE embankment especially for the frequency of input motion close to the natural frequency of system.

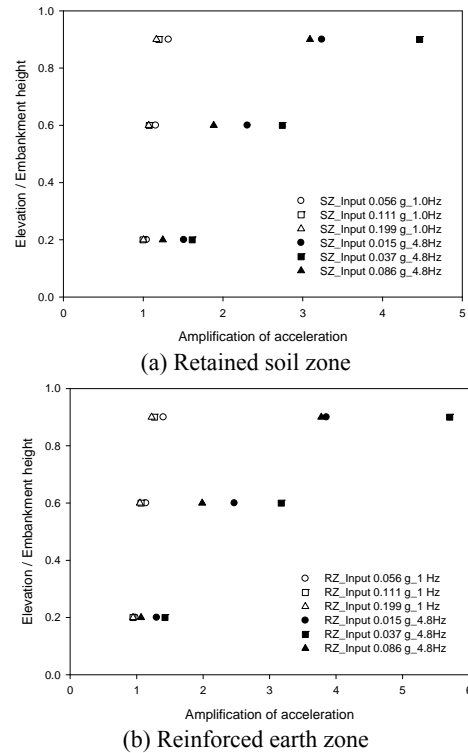
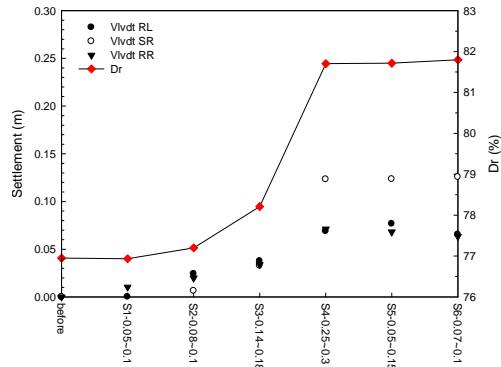


Figure 11 Relationships between the amplification of acceleration and the elevation.

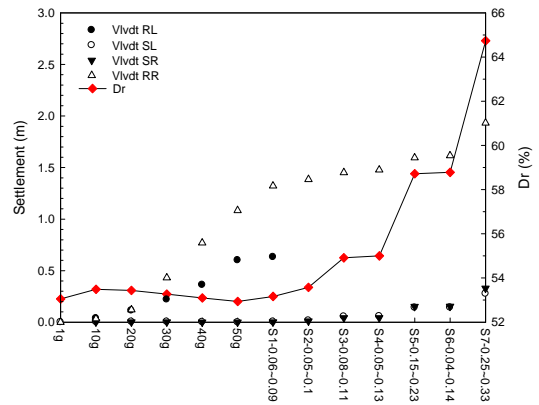
3.3 Deformation of GRE Embankment

Figures 12(a) to 12(g) show the accumulated settlements and the change of related density during the tests. The x-axis describes the information of seismic events including the number of event, maximum input acceleration and the maximum acceleration response. The positive acceleration is the direction toward the right-side of model shown in Figure 3. Therefore, the movement of right-side reinforced earth zone is usually much more than that of left-side and leading to more settlement. Most settlement occurs after three 1 Hz shakings and the deformation increases with increasing amplitude of input motion. The shaking loadings with frequency of 4.8 Hz do not lead to significant settlement. It can be observed that the settlement of retained soil zone is larger than that of reinforced earth zone. Table 4 summarizes the peak base acceleration (PBA) of GRE embankment and the normalized settlements by height of each event with frequency of 1 Hz. The effect of different parameters on the settlement of GRE embankment is discussed as follows:

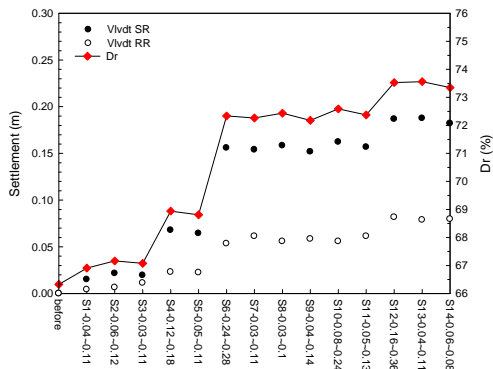
The settlements of models 1:1-N10-T112-L70, 1:0.5-N10-T112-L70, 1:1-N16-T112-L70 and 1:0.5-N16-T112-L70 were close and equal to about 3 % of height. It means that when the reinforcement strength is high enough, the reinforcement spacing of 0.5 m or 0.8 m and the inclination of 45 degrees or 63.4 degrees would not affect the settlement significantly. Generally speaking, the 1 Hz input motions of 0.06 g, 0.13 g and 0.23 g would result in settlement of 0.134 %, 0.500 % and 1.156 % of height, respectively.



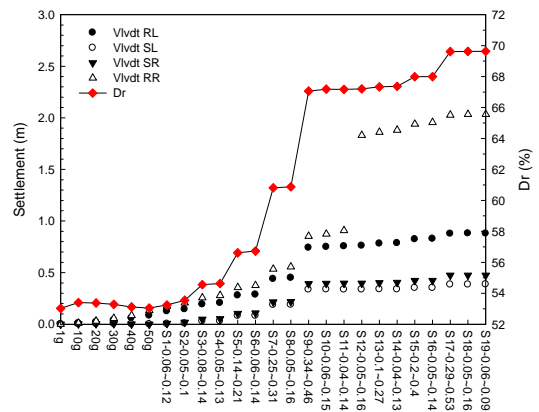
(a) 1:1-N10-T112-L70



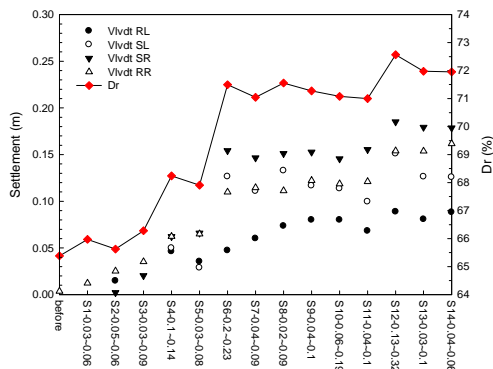
(e) 1:0.5-N10-T2.5-L30



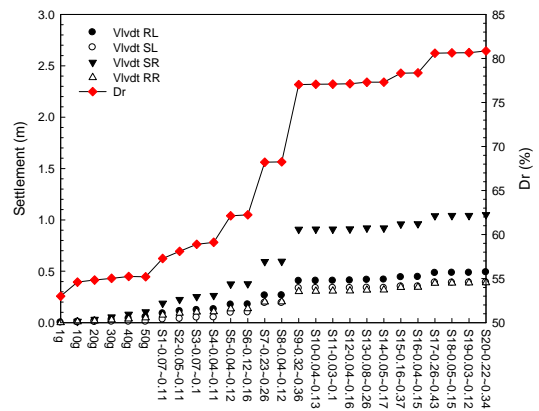
(b) 1:0.5-N10-T112-L70



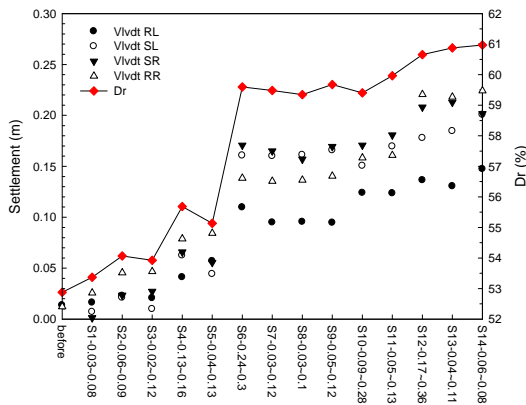
(f) 1:0.5-N10-T2.5-L50



(c) 1:1-N16-T112-L70



(g) 1:0.5-N10-T2.5-L70



(d) 1:0.5-N16-T112-L70

Figure 12 Accumulated settlements of tested models

For the models 1:0.5-N10-T112-L70 and 1:0.5-N10-T2.5-L70, the factor of safeties for breaking failure of reinforcement material are about 4.26 and 0.09. As shown in Figure 13, significant ruptures of reinforcement were observed from model 1:0.5-N10-T2.5-L70 after a series shaking events. The settlement of 1:0.5-N10-T2.5-L70 is more than twice as large as that of 1:0.5-N10-T112-L70 when the models subjected to the same PBA. With the same geometry and reinforcement arrangement, the GRE embankment using insufficient reinforcement strength would lead to internal instability failure and a large settlement.

Table 4 Settlement of GRE embankment subjected to 1 Hz loadings

Test No.	Seismic event (1 Hz)	Max. IBA (g)	Normalized settlement by height (%)			
			RL	SL	SR	RR
1:1-N10-T112-L70	S2	0.08	0.375	-	0.088	0.125
	S3	0.14	0.125	-	0.375	0.125
	S4	0.25	0.375	-	1.125	0.500
1:0.5-N10-T112-L70	S2	0.06	-	-	0.125	0.025
	S4	0.12	-	-	0.625	0.125
	S6	0.24	-	-	1.125	0.375
1:1-N16-T112-L70	S2	0.05	0.375	0.250	0.075	0.125
	S4	0.10	0.625	0.750	0.500	0.375
	S6	0.20	0.125	1.250	1.125	0.500
1:0.5-N16-T112-L70	S2	0.06	0.075	0.125	0.250	0.250
	S4	0.13	0.250	0.625	0.500	0.375
	S6	0.24	0.625	1.250	1.250	0.625
1:0.5-N10-T2.5-L30	S3	0.08	-	0.500	0.375	0.875
	S5	0.14	-	1.000	1.375	1.375
	S7	0.26	-	1.625	2.250	3.875
1:0.5-N10-T2.5-L50	S3	0.08	0.625	0.250	0.375	0.625
	S5	0.14	0.875	0.625	0.625	1.000
	S7	0.25	1.875	1.250	1.375	2.000
1:0.5-N10-T2.5-L70	S3	0.07	0.125	0.125	0.375	0.125
	S5	0.12	0.500	0.625	1.375	0.375
	S7	0.23	1.125	1.125	2.750	0.750

* The symbol “-” means the sensor was out of the function.



Figure 13 Breakage of reinforcement material

Based on design guidelines, reinforcement length should be at least 70 % of height for reinforced earth structure. Three models with very weak reinforcement strength of 2.5 kN/m, 1:0.5-N10-T2.5-L30, 1:0.5-N10-T2.5-L50 and 1:0.5-N10-T2.5-L70, were conducted to simulate the worst design conditions and to investigate the deformation of GRE embankment with not enough reinforcement strength and length under a series of shakings. It can be seen in Figure 12(e) that a very large settlement occurred during spinning the centrifuge from 1 g to 50 g and they were about 1.2 m, 0.19 m and 0.13 m for model 1:0.5-N10-T2.5-L30, 1:0.5-N10-T2.5-L50 and 1:0.5-N10-T2.5-L70, respectively. Figure 14(a), 14(b) and 14(c) show the model profiles before and after the test. The black solid line is the original profile and the location of reinforcement materials. The red solid and dashed lines sketched the deformed model at different profiles. The reinforcement length of 30% of height is too short and would lead to the external instability of structure for both side of reinforced earth zone which were moving outward after test shown in Figure 14(a). If settlement of 30% of height was a threshold value to determine the failure of structure as shown in Figures 14(a) and 14(b), models with the longer reinforcement can sustain the more number of seismic loadings.

Two LVDTs setup in front of the left facing were named LT (left-top) and LM (left-middle). At the right facing, the other two were named RT (right-top) and RM (right-middle). The maximum

horizontal displacement occurs at the middle of slope facing. During the test, settlement and horizontal displacement occurred at the same time. It is difficult to monitor a point with outward and downward movements by a LVDT. The methods of photogrammetry may be a solution of this problem in the future.

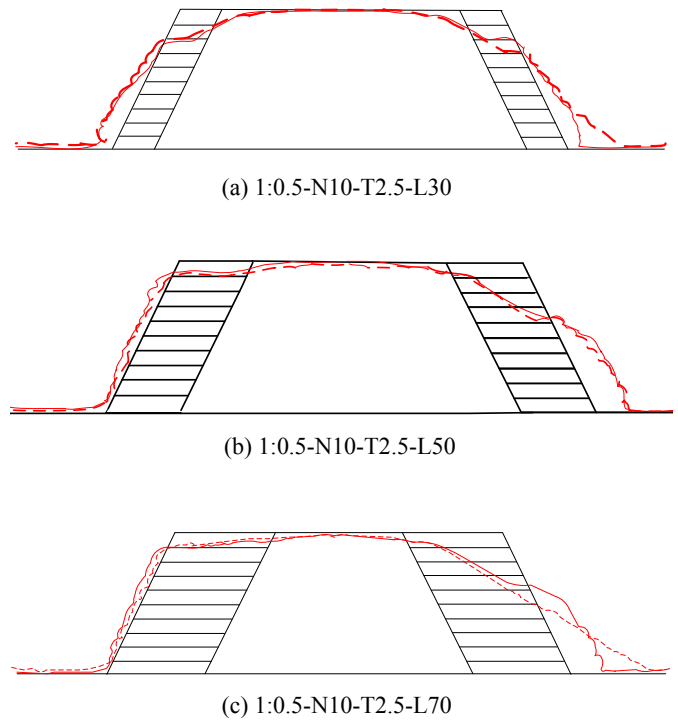


Figure 14 Deformation of GRE embankment for different reinforcement length

4. CONCLUSIONS

A series of centrifuge shaking table tests was performed to investigate the seismic response of geosynthetic reinforced earth embankment with different geometry and reinforcement arrangement. Several conclusions can be drawn as follows.

1. The natural frequency of an 8 m-high GRE embankment is about 5.7Hz. The arrangement of reinforcement and the inclination of slope facing do not affect the natural frequency significantly.
2. The amplification of acceleration increases with the increasing elevation and the increasing frequency of input motion. The influences of elevation of embankment and frequency of input motion on amplification are not considered in the current design guidelines. The design results would underestimate the seismic response at the top portion of the GRE embankment.
3. If the GRE embankment has enough reinforcement strength, the reinforcement spacing of 0.5 m or 0.8 m and the inclination of 45 degrees or 63.4 degrees would not affect the settlement significantly.
4. Insufficient reinforcement strength would lead to internal instability failure and a large settlement. The external instability would occur for the GRE embankment using too short reinforcement length.

To monitor a point at slope facing with outward and downward movements by a LVDT is very difficult. It is unfortunate that the used rigid container does not have a visual window for the image processing method. The methods of photogrammetry may be a solution of this problem in the future. Only seven models were tested in this manuscript, more tests and parametric studies would be performed in advanced to give more indications of reliability of GRE embankment in the field.

5. ACKNOWLEDGEMENTS

The authors would like to express their gratitude for the financial and technical supports from the National Center for Research on Earthquake Engineering and National Science Council (NSC 101-2221-E-492-027 and NSC 102-2221-E-008-116). These supports make this study and the future researches possible.

6. REFERENCES

- Chen, H.T., Hung, W.Y., Chang, C.C., Chen, Y.J and Lee, C.J. (2007). "Centrifuge modeling test of a geotextile-reinforced wall with a very wet clayey backfill". *Geotextiles and Geomembranes*. Vol. 25, Issues 6, pp 346-359.
- Elias, V., Christopher, B.R., and Berg, R.R. (2001). "Mechanically stabilized earth walls and reinforced soil slopes design and construction guidelines." Report No. FHWA-NHI-00-043, National Highway Institute, Federal Highway Administration, Washington, D.C. March.
- Hu, Y., Zhang, G., and Lee, C.F. (2010). "Centrifuge modeling of geotextile-reinforced cohesive slopes". *Geotextiles and Geomembranes*. Vol. 28, Issues 1, pp 12-22.
- Hung, W.Y., (2008). "Breaking failure behavior and internal stability analysis of geosynthetic reinforced earth walls," Ph. D. Thesis, National Central University, Jhongli, Taiwan.
- Law, H., Ko, H.Y., Goddery, T. and Tohda, J., (1992). "Prediction of the performance of a geosynthetic-reinforced retaining wall by centrifuge experiments," *Geosynthetic-Reinforced Soil Retaining Walls* (ed. Wu, J.T.H.), Balkema, Rotterdam, pp. 347-360.
- Lee, S.H., (1997). "Post-earthquake investigation on several geosynthetic-reinforced soil retaining walls during the Hanshin-Awaji earthquake of Japan". *Modern Construction*. No. 210, pp 24-49. (In Chinese)
- Leshchinsky, D. and Han, J., (2004). "Geosynthetic reinforced multitiered walls," *Journal of Geotechnical and Geoenvironmental Engineering*, Vol. 130, No. 12, pp. 1225-1235.
- Ling, H.I., Leshchinsky, D. and Chou, N. S. (2001) "Post-earthquake investigation on several geosynthetic-reinforced soil retaining walls and slopes during the Ji-Ji earthquake of Taiwan". *Soil Dynamics and Earthquake Engineering*. Vol. 21, Issues 4, pp 297-313.
- Lord Jr, E. (1987). "Geosynthetic/soil studies using a geotechnical centrifuge," *Geotextiles and Geomembranes*, Vol. 6, pp.133-156 (1987).
- NCMA (2010). *Design manual for segmental retaining walls*, National Concrete Masonry Association Herndon, VA.
- Nova-Roessig and Nicholas Sitar, (2010). "Centrifuge model studies of the seismic response of reinforced soil slopes". *Journal of Geotechnical and Geoenvironmental Engineering*. Vol. 132, Issues 3, pp 388-400.
- Nova-Roessig, L., and Sitar, N. (2006). "Centrifuge model studies of the seismic response of reinforced soil slope". *Journal of Geotechnical and Geoenvironmental Engineering*, ASCE, Vol. 132, Issues 3, pp 388-400.
- Viswanadham, B.V.S., and Kong, D. (2009). "Centrifuge modeling of geotextile-reinforced slopes subjected to differential settlements". *Geotextiles and Geomembranes*. Vol. 27, Issues 2, pp77-88.
- Zhang, W., Lai, Z., and Xu, G., (2000). "Centrifuge modeling of geotextile-reinforced cohesionless soil retaining walls," *China Civil Engineering Journal*, Vol. 33, No. 3, pp. 84-91.
- Zornberg, J.G., Mitchell, J.K. and Sitar, N., (1997). "Testing of reinforced slopes in a geotechnical centrifuge," *Geotechnical Testing Journal*, GTJODJ, Vol. 20, No. 4, pp. 470-480.
- Zornberg, J.G., Sitar, N. and Mitchell, J. K., (1998). "Performance of geosynthetic reinforced slopes at failure," *Journal of Geotechnical and Geoenvironmental Engineering*, Vol.124, No.8, pp.670-683.